Advances in Basic and Applied Sciences 1 (2023) 13-20

Advances in Basic and Applied Sciences

journal homepage: https://abas.journals.ekb.eg/

Enhancement of the photocatalytic Degradation of methylene blue by sonication

Esam Alarfaj*, Bedor Alyahya

Physics Department, College of Science, Qassim University, Buraydah 5145, Saudi Arabia

ARTICLE INFO

Article history:
Received 21 February 2023
Accepted 7 March 2023
Available online 3 June 2023

doi: 10.21608/ABAS.2023.195357.1007

Keywords: TiO_2, photocatalysis, sonophotocatalysis, photocatalytic degradation

ABSTRACT

This study investigates the effect of sonication on the degradation activity of MB in an aqueous solution. This process is in the presence of high-quality nanoparticles (NPs) TiO_2 catalysts and under UV- light irradiation. It was under taken using X-ray diffraction (XRD), scanning electron microscopy (SEM) and UV-Vis spectrophotometer. XRD analysis confirmed the presence of pure anatase phase and the calculated crystallite size of about 54 nm. The band gap energy was found to be 3.2 eV, which corresponds to anatase phase. The degradation activities of methylene blue (MB) were evaluated for photo catalysis and sonophotocatalysis processes separately. According to the results obtained, it was shown that the degradation of MB during sonophotocatalysis of TiO_2 catalysts was accomplished in a shorter time, which was due to the enhancement of formation of free hydroxyl radicals during sonication. The enhancement of photocatalytic degradation of methylene Blue was significant compared to performing just photo catalysis.

1. Introduction

Different organic pollutant dyes generated from textile industries are deemed to be significant environmental wastewater. When these pollutants are discharged into water, they cause a great risk to the ecological balance in the environment. So, several reports have focused on the development of wastewater treatment and remediation techniques to remove, absorb, or degrade toxic dye pollutants from wastewater. These techniques are generally based on physical, chemical and biological methods such as adsorption, coagulation, membrane process, and advanced oxidation processes are currently available for treating dye wastewater. Advanced oxidation processes (AOPs) have received a great attention because it constitutes a promising methods developed to remove persistent organic pollutants. The main types of AOPs include photolysis, photocatalysis, sonolysis, sonophotocatalysis and Fenton-based reactions [1,2]. It has been shown in many researches that sonophotocatalysis is a promising advanced oxidation method for the degradation of organic pollutant dyes, which involves the combination of ultrasound waves and semiconductor photocatalyst to improve and enhance the degradation performance [2–6].

Metal oxide semiconductors have been extensively used as

* **Corresponding author E-mail:** *issaam@gmail.com*

a catalyst in photocatalytic, particularly as heterogeneous photocatalysts in the degradation of pollutant dyes. Their band gap energies are in the UV or visible light region [7]. Among the various oxide semiconductor catalysts, TiO_2 is the most commonly applied material due to its biological and chemical inertness, stability, non-toxicity, low cost, water insolubility under most environmental circumstances and stability against photochemical corrosion [7–10].

Several reports have investigated the photocatalytic and sonophotocatalytic degradation rates of different organic pollutants in the presence of TiO_2 catalyst. Jelic et al. [11] reported that the influence of in situ sonication on photocatalytic degradation resulted in a significant enhancement of carbamazepine (CBZ) degradation. Wu et al. [12] studied the removal of reactive red 2 dyes during sonocatalysis, photocatalysis and sonophotocatalysis processes using TiO_2 NPs. They observed that the degradation rate was faster in the presence of sonication. The study of Taghizadeh et al. [13] showed that the combination of sonolysis and photocatalysis, in the presence of TiO_2 NPs under UV irradiation, leads to faster removal of chitosan dyes than the individual process.

Nonetheless, very few reports have been carried out on the study of methylene blue (MB) degradation using TiO_2 NP. Consequently, in our study. The evaluation of MB upon photocatalytic and sonophotocatalytic oxidation under UV light irradiation using TiO_2 NPs is studied. The characteristics of TiO_2 NPs were characterized using X-ray diffraction (XRD), spectrophotometer, scanning electron microscopy (SEM) and UV-Vis Spectroscopy

2. Experimental

2.1 Catalyst characterization

The XRD patterns of the TiO_2 NPs were obtained at room temperature using a diffractometer Shimadzu, model lab X 6000 with Cu Kα radiation (λ = 0.1514 nm) in the range of 20–75. SEM was conducted using an INSPECT S50-SEM with a working distance of 23.6 mm and 24.9, acceleration 15 kV voltage and emission current 94.7. UV–Vis absorbance spectra were recorded using a SHIMADZU UV-2600 Spectrophotometer.

2.2 Photocatalytic and sonophotocatalytic testing

We conducted two tests to evaluate photocatalysis (catalyst + UV) and sonophotocatalysis (catalyst + UV + US) degradation of MB. For nanoparticles TiO_2, MB ($C_{16}H_{18}N_3S$) was used as an organic dye to evaluate the ability of the nanoparticles to degrade organic compounds in aqueous solution. 10-ppm MB was dissolved in 100 ml volume of distilled water to obtain a diluted solution. The photocatalysis process was performed under a UV lamp on a home-made photoreactor system at 42°C (Fig. 1a). In this experiment, UV lamp, with 6 W and wavelength 366 nm) was placed 10 cm away from the reactor. Air bubbles were added onto the solution of TiO_2 nanoparticles. 0.5 g/L of high-quality TiO2 nanoparticles was used and mixed for 10 min using a magnetic stirrer and at 32°C then 20 ml of MB aqueous solution was added to the catalyst. After the UV irradiation, the suspended particles were removed out and centrifuged at 60000 RPM for 20 min. Some of the MB was taken from the top of the centrifuged sample into the vial. During the photocatalytic degradation, the catalyst was removed from the solution at different times until the complete degradation of MB was reached.

A sonophotocatalytic reactor was assembled by placing the photocatalytic reactor in the sonication bath, as shown in Fig. 1b. The US power was 130 Watts and the frequency 40 KHz. During the sonophotacalylsis degradation, the catalysis was taken from the solution at different times until the complete degradation of MB was reached, which were 180 min and 420 min for TiO_2 NPs, respectively. The initial pH of TiO_2 nanoparticles, in aqueous solution, is 8.04.

3. Results and discussion

3.1 Structural analysis

Fig. 2 depicts the XRD pattern, of TiO_2 NPs in the 2θ range of 20–75. The peak positions of the sample appear at 2θ = 24.5, 36, 37, 37.8, 47.2, 53, 54.5, 61.8, 67.8, 69.4, and 74.2 corresponding to the (101), (103), (004), (112), (200), (211), (105), (204), (116), (220), and (215) crystal planes, respectively. The diffraction peaks indicate the anatase phase [14–18]. However, the rutile and brookite phases are completely missing in the high-quality TiO_2 NPs, which agrees with previous studies [19].

The crystalline size D of anatase TiO_2 NPs was estimated, by taking intensive (101) peak in the XRD spectrum, using Scherrer's formula [20]:

$$D = k\lambda/\beta\cos\theta \qquad (1)$$

where k = 0.9 is the shape factor, λ is the X-ray wavelength (λ=1.5406 Å), β is the full width at half maximum (FWHM) in rad and θ is the Bragg angle. The calculated crystallite size for the high-quality TiO_2 used in our study is about 54 nm.

3.2 Optical analysis

Fig. 3 depicts the optical absorption spectrum of the TiO_2 NPs within a wavelength range from 300 nm to 700 nm. The curves show strong absorption in the UV region recorded at

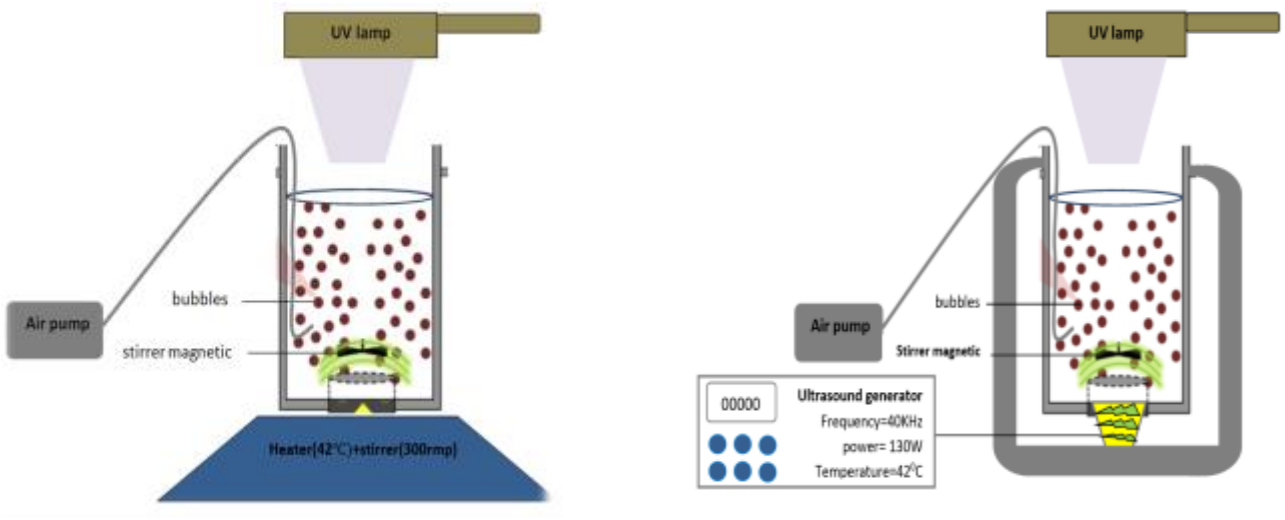

Fig. 1: Experimental set-up of (a) photocatalytic and (b) sonophotocatalytic reactors

320 nm and 332 nm for TiO_2 NPs, respectively, which is due to the absorption of light caused by the excitation of electrons from the valence band to the conduction band of TiO_2[24].

The value of optical band gap energy can be estimated using the Tauc equation extracted from absorption spectra using Tauc equation [25,26]:

$$(\alpha h\nu) = k(h\nu - E_g)^m \quad (2)$$

Where, $h\nu$ represents incident photon energy, α is the absorption coefficient, k proportionality constant and E_g is bandgap energy and the m value depends on the electronic transition, when = 1/2, the semiconductor had a direct band gap, while when = 2, the semiconductor had an indirect band gap. Fig. 4 illustrate αhν versus photon energy for the indirect transition of TiO2 NPs. The band gap energy values were obtained by extrapolating the linear part of each curve onto the energy axis. The indirect band gap value is 3.2 eV for the samples. Indeed, the literature reports a 3.2 eV value for the anatase phase [27,28], indicating that the high-quality TiO2 NPs used in this study with anatase phase follow an indirect type transition which is agree with previous studies [29,30].

3.3 Degradation activity

The degradation activities of TiO_2 NPs were evaluated by degradation of MB in aqueous solution under UV-light irradiation (photocatalysis process) and in situ sonication (sonophocatalysis process). The UV-Vis absorbance spectra of liquid samples catalyzed by the TiO_2 NPs during the photocatalysis process are illustrated in Fig. 3. The absorbance spectra showed strong absorbance in the visible region with a maximum absorption peak of MB displayed at the wavelength of 664 nm when catalyzed by NPs. Further, the optical absorbance of MB dye becomes almost neglected after 240 min in the presence of NPs catalyst (Fig. 5).

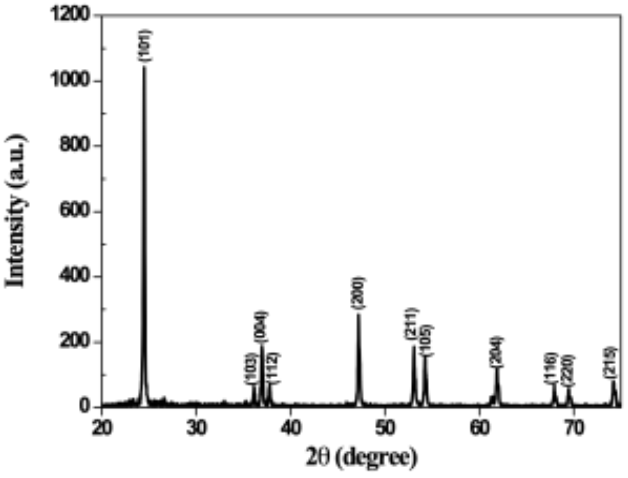

Fig. 2: XRD pattern of TiO_2 NPs

Fig. 6 displays the degradation activity as a function of UV irradiation time during the photocatalysis process using TiO_2 NPs. As shown in this figure, the degradation activity increases with irradiation time. The degradation efficiency of MB through 240 min reached above 91.15% when we used TiO_2 NPs as catalyst. Sahoo et al. [33] estimated a degradation efficiency of MB about 93% within 180 min of UV irradiation, using 2 g/L of a commercial TiO_2 NPs catalyst. Dariani et al. [34] showed that the complete decomposition of MB occurred in 5 h UV irradiation time and the degradation efficiency was 100%, using 1 g of TiO_2 NPs as catalyst and 5ppm of initial MB concentration.

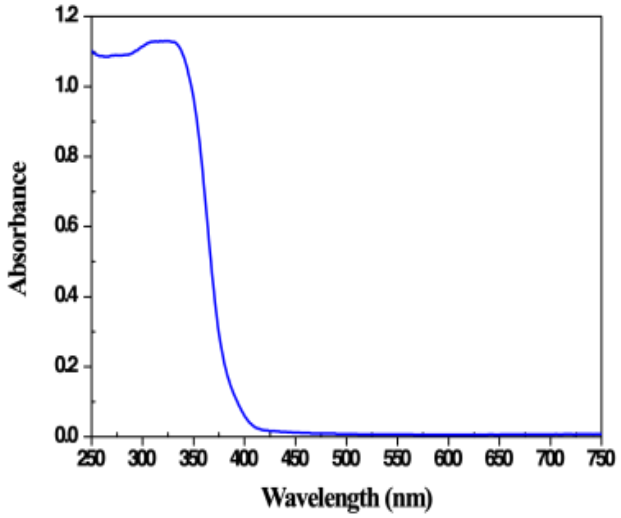

Fig. 3: UV–vis absorbance spectra of TiO_2 NPs

However, they found that the increase in MB initial concentration (20-ppm) decreased the degradation efficiency from 100% to 80%. The photocatalytic activity of MB, using anatase Titania nanoparticles, was estimated in the study by Aghareed et al. [35]. The experimental results exhibited that MB degradation was achieved 94.56% through 90 min; obtained when they used 5-ppm MB dye, 0.1 g of TiO_2 catalyst and pH 12.6 of aqueous solution. The difference in the dye degradation values is mainly due to the different in various experimental parameters such as pH, amount of catalyst, dye concentration and reaction temperature [36–39]. Additionally, the curve corresponding to the degradation activity of MB organic dye using TiO_2 thin film revealed that the photocatalytic activity was ~92.9% and MB color is almost removal within 750 min, which is approximately 3 times greater than that obtained after a complete degradation using TiO_2 NPs as a catalyst. This is attributed to a higher surface area of NPs form, conducting to enhance a photocatalytic degradation [36,40]. Chan et al. [41] reported that using pure poreless TiO_2 film to degrade MB, a maximum photocatalysis activity was only about 30% after 6h of UV illumination. Whereas, mesoporous film increased the photocatalysis activity up to 80%, this was attributed to the high active surface area, leading to an increase the hydroxyl radicals. Further, radicals are responsible for absorbing the MB dyes in the aqueous solution. Fig. 7 illustrates the UV-Vis absorbance spectra of liquid samples catalyzed during the sonophotocatalysis process using the TiO2 NPs (Fig. 5.). The absorbance spectra showed strong absorbance in the visible region catalysts and the highest absorbance peak recorded in wavelength 664 nm. Additionally, a decrease in absorption peaks was observed with an increase in UV-light irradiation time and the MB degradation was almost completed whiting 180 min using NPs. The percent degradation versus irradiation time of MB dye using TiO_2 NPs during the sonophotocalysis process is depicted in Fig. 8.

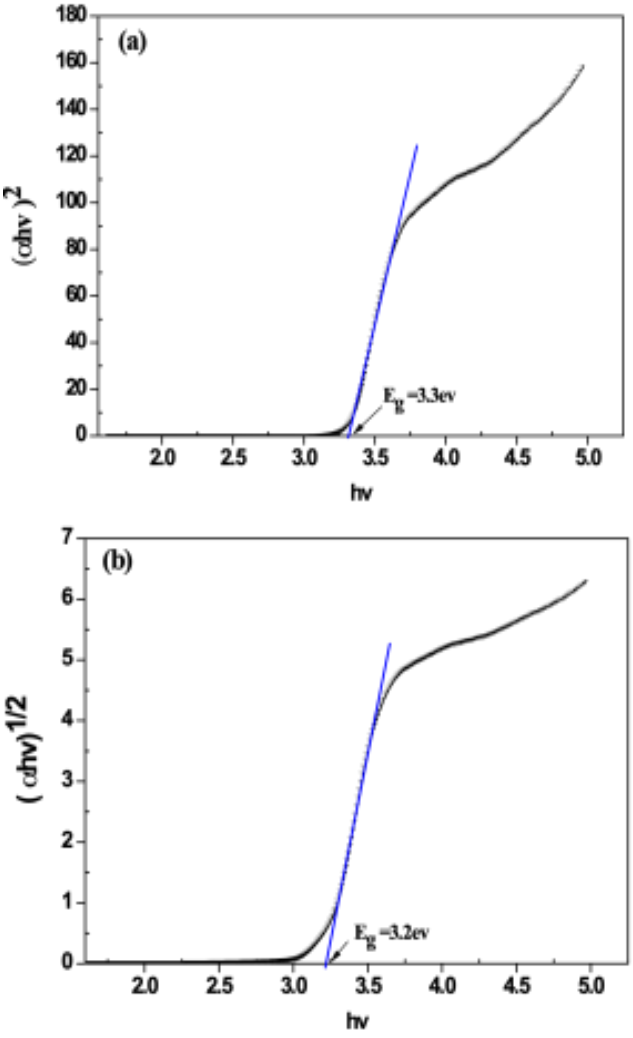

Fig. 4: Calculation of indirect bang gap energy of TiO_2 NPs

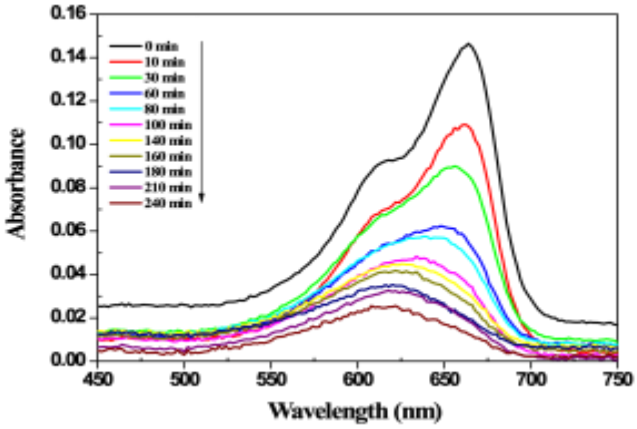

Fig. 5: UV-vis absorption spectra of MB solution catalyzed by TiO_2 NPs during the photocatalysis process.

As shown in this figure, a complete removal of pollutant dyes is achieved after 180 min using NPs, which indicated that the degradation rate was faster than that obtained during the photocatalysis process. Moreover, the percent degradation of the dye is above 99% after complete removal of MB dye for both catalysts. Indeed, the rate of degradation during the sonophotacatalysis process depends on various experimental parameters, such as US power and US frequency [42–44]. The choice of optimum degradation parameters leads to a high degradation rate in a shorter time. Several studies were conducted on the sonophotocatalytic degradation of different dyes such as MB, 1,4-dichlorobenzene, Congo red and methyl orange, acid red 88, acid orange, Eosin B and Rhodamine B, using TiO_2 NPs catalyst [5,45-48]. The obtained results showed an enhancement and improved degradation efficiency after addition a sonication, and a complete degradation took a shorter time with the exposure to in situ UV-light and ultrasound action.

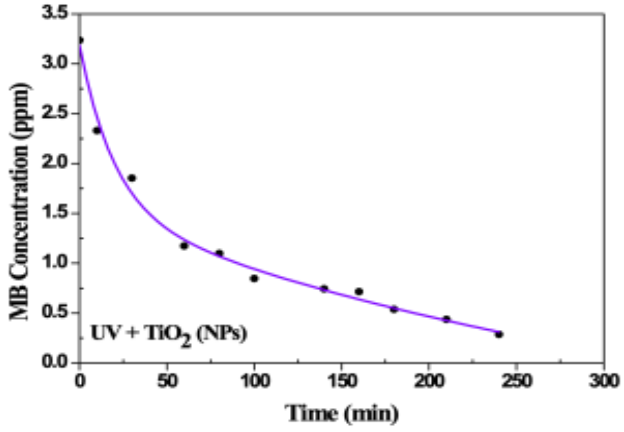

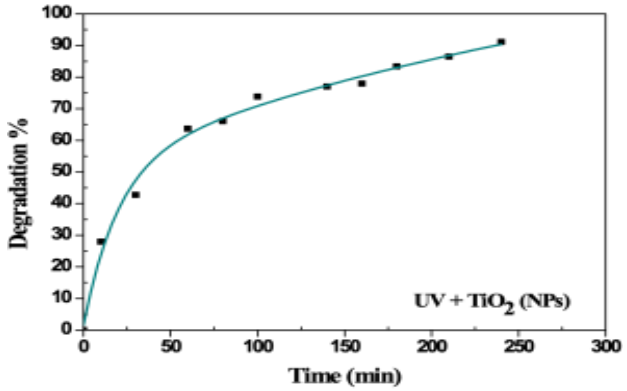

Fig. 6 Degradation activity vs. irradiation time during the photocatalysis process.

It can be attributed to the increased production of a greater number of free hydroxyl radicals which are responsible of dye decomposition [49]. Furthermore, the combination of pure anatase phase with the high specific surface area leads to enhance the photocatalytic activity of TiO_2 NPs [50]. The higher photocatalytic activity of anatase TiO_2 NPs can be attributed to an increase in the formation of radicals due to the lower electron-hole recombination probability [51].

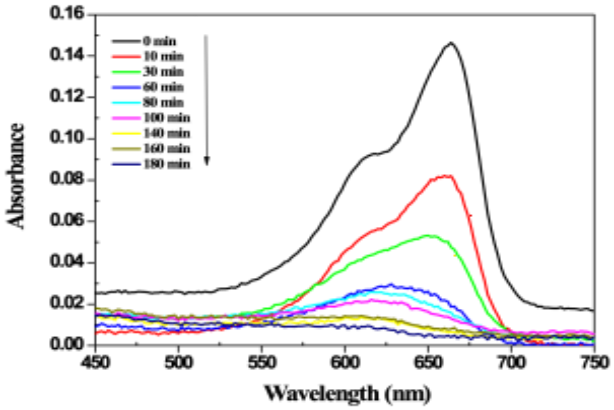

Fig. 7: UV-Vis absorption spectra of MB solution catalyzed by TiO_2 NPs during the sonophotocatalytic process.

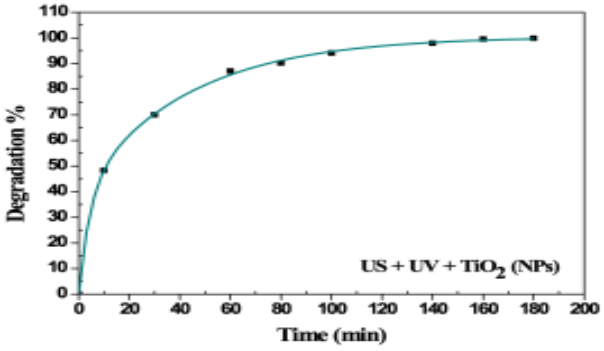

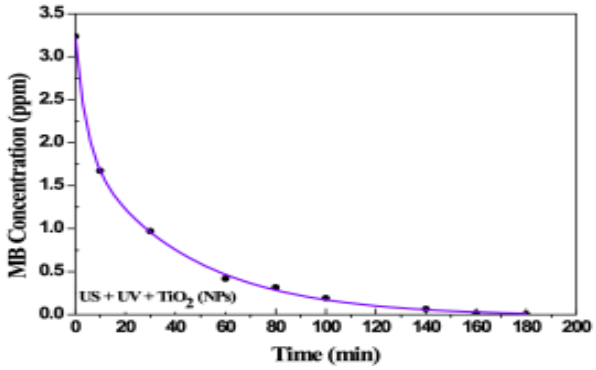

Fig. 8: Degradation activity vs. irradiation time during sonophotocalysis process

Conclusions

In this work, the degradation efficiency was evaluated by the decomposition of MB under UV-light irradiation using anatase TiO_2 NPs used as catalyst during photocatalysis and sonophotocatalysis processes. The degradation efficiency value of MB in aqueous solution using NPs as the catalyst during the photocatalysis process is almost 91.15% through UV-light irradiation time. This is mainly attributed to the high area surface, which conducted to generate more radicals. The influence of in situ sonication on the degradation activity of MB dyes using TiO_2 NPs was also studied. It was observed that the degradation rate of MB during sonophotocatalysis was faster than the photocatalysis process of TiO_2 which was attributed to the enhancement of formation of free hydroxyl radicals during sonication.

References

1. Z. Chenga, X. Quan, Y. Xiong, L. Yang, Y. Huang. Synergistic degradation of methyl orange in an ultrasound intensified photocatalytic reactor. Ultrasonics Sonochemistry 19 (2012) 1027–1032.
2. J. Madhavana, P.S. S. Kumara, S. Anandan, F. Griesera, M. Ashokkumar. Degradation of acid red 88 by the combination of sonolysis and photocatalysis. Separation and Purification Technology 74 (2010) 336–341.
3. A. Nakajima, M. Tanaka, Y. Kameshima and K. Okada. Sonophotocatalytic Destruction of 1,4-Dioxane in Aqueous Systems by HF-Treated TiO2Powder.Journal of Photochemistry and Photobiology A: Chemistry 167 (2004) 75–79.
4. C. Berberidou, I. Poulios, N. P. Xekoukoulotakis and D. Mantzavinos. Sonolytic, Photocatalytic and Sonophotocatalytic Degradation of Malachite Green in Aqueous Solutions. Applied Catalysis B: Environmental 74 (2007) 63–72.
5. N.J. Bejarano-Perez and M. Fidel Suarez-Herrera. Sonophotocatalytic Degradation of Congo Red and Methyl Orange in the Presence of Tio2 as a Catalyst. Ultrasonics Sonochemistry 14 (2007) 589–595.
6. M. May-Lozano, V. Mendoza-Escamilla, E. Rojas-García, R. Lopez-Medina, G. RivadeneyraRomero and S. A. Martinez-Delgadillo. Sonophotocatalytic Degradation of Orange II Dye using Low-cost Photocatalyst. Journal of Cleaner Production 148 (2017) 836–844.
7. M. M. Khan, S. F. Adil, A. Al-Mayouf. Metal oxides as photocatalysts. Journal of Saudi Chemical Society (2015) 462–464.
8. M. Rauf, M. Meetani, A. Khalee and A. Ahmed. Photocatalytic degradation of methylene Blue using a Mixed Catalyst and Product analysis by LC/MS. Chemical Engineering Journal 157 (2010) 373–378.
9. A. M, Tayeb, and D. S. Hussein. Synthesis of TiO2 Nanoparticles and Their Photocatalytic Activity for Methylene Blue. American Journal of Nanomaterials 3(2015) 57–63.
10. K. Nakata and A. Fujishima. TiO2 Photocatalysis: Design and Applications. Journal of Photochemistry and Photobiology C: Photochemistry Reviews 13 (2012) 169 – 189.
11. A. Jelic, I. Michael, A. Achilleos, E. Hapeshi, D. Lambropoulou, M. Petrovic, D. FattaKassinos, D. Barcelo, S. Perez. Transformation products and reaction pathways of carbamazepine during photocatalytic and sonophotocatalytic treatment. Journal of Hazardous Materials 263 (2013) 177–186.
12. CH. Wu, CH. Yu. Effects of TiO2 dosage, pH and temperature on decolorization of C.I. Reactive Red 2 in a UV/US/ TiO2 system. Journal of Hazardous Materials 169 (2009) 1179–1183.
13. M. T. Taghizadeh and R. Abdollahi. Sonolytic, Sonocatalytic and Sonophotocatalytic Degradation of Chitosan in the Presence of TiO2 Nanoparticles. Ultrasonics Sonochemistry 18 (2011) 149–157
14. H. M. Chenari, C. Seibel, D. Hauschild, F. Reinert, H. Abdollahian. Titanium Dioxide Nanoparticles: Synthesis, X-Ray Line Analysis and Chemical Composition Study. Materials Research 6(2016)1319–1323.
15. E. Al-Hetlani, M.O. Amin, M. Madkour. Detachable photocatalysts of anatase TiO2 nanoparticles: Annulling surface charge for immediate photocatalyst separation. Applied Surface Science 411 (2017) 355–362.
16. N. Sofyan, A. Ridhova, A. H. Yuwono and A. Udhiarto. Preparation of anatase TiO2 nanoparticles using low hydrothermal temperatures for dye-sensitized solar cell. IOP Conf. Series: Materials Science and Engineering 316 (2018) 012055.
17. D. Reyes-Coronado, G. Rodr´ıguez-Gattorno, M. E. Espinosa-Pesqueira, C. Cab, R. de. Coss and G. Oskam. Phase-pure TiO2 nanoparticles: anatase, brookite and rutile. Nanotechnology 19 (2008) 145605 (10pp).
18. Y. F. You, C.H. Xu, S.S. Xu, S. Cao, J. P. Wang, Y.B. Huang, S.Q. Shi. Structural characterization and optical property of TiO2 powders prepared by the sol–gel method. Ceramics International 40 (2014) 8659–8666.

20. Z. M. Abou-Gamra, M. A. Ahmed. The synthesis of mesoporous TiO2–curcumin nanoparticles for photocatalytic degradation of methylene blue dye. Journal of Photochemistry & Photobiology, B: Biology 160 (2016) 134–141.
21. Y. C. Chen. The effect of Ultrasound on the Photo Catalytic Degradation of Organic Compounds. Master of Science (2002). National Chung-Hsing University, Taiwan.
22. L. Zhang, L. Han, P. Hu, L. Wang, and S. Dong. TiO2 Nanotube Array: Intrinsic Peroxidase Mimetics. Society of Chemistry 2013.
23. K. Cheng, D. Cao, F. Yang, L. Zhang, Y. Xu and G. Wang. Electrodeposition of Pd nanoparticles on C@TiO2 nanoarrays: 3D electrode for the direct oxidation of NaBH4. Journal of Materials Chemistry, 2012, 22, 850–855.
24. G. Govindasamy, P. Murugasen, S. Sagadevan. Investigations on the Synthesis, Optical and Electrical Properties of TiO2 Thin Films by Chemical Bath Deposition (CBD) method. Materials Research. 2016; 19(2): 413–419.
25. R. Zouzelka, Y. Kusumawati, M. Remzova, J. Rathousky, T. Pauporté. Photocatalytic Activity of porous multiwalled carbon nanotube-TiO2 composite layers for pollutant degradation. Journal of Hazardous Materials 317 (2016) 52–59.
26. D. Komaraiah, P. Madhukar, Y. Vijayakumar, M. V. R. Reddy and R. Sayanna. Photocatalytic Degradation Study of Methylene Blue by Brookite TiO2 Thin Film Under Visible Light Irradiation. Materials Today: Proceedings 3 (2016) 3770–3778.
27. C. Yu, J. Park. Thermal annealing synthesis of titanium-dioxide nanowire–nanoparticle hetero-structures. Journal of Solid State Chemistry 183 (2010) 2268–2273.
28. R. Kavitha, S. Meghani, V. Jayaram. Synthesis of titania films by combustion flame spray pyrolysis technique and its characterization for photocatalysis. Materials Science and Engineering B 139 (2007) 134–140.
29. S. Valencia, J. M. Marín and G. Restrepo. The study of the Bandgap of Synthesized Titanium Dioxide Nanoparticules Using the Sol-Gel Method and a Hydrothermal Treatment. The Open Materials Science Journal 4(2010) 9–14.
30. D. Reyes-Coronado, G. Rodr´ıguez-Gattorno, M. E. Espinosa-Pesqueira, C. Cab, R. de. Coss and G. Oskam. Phase-pure TiO2 nanoparticles: anatase, brookite and rutile. Nanotechnology 19 (2008) 1–10.
31. K. M. Reddy, S. V. Manorama, A. R. Reddy. Bandgap studies on anatase titanium dioxide nanoparticles. Materials Chemistry and Physics 78 (2002) 239–245.
32. K. F. Azizi, M.- M. Bagheri- Mohagheghi. The effect of solution flow rate and substrate temperature on structural and optical properties of TiO2 films deposited by spray pyrolysis technique. Thin Solid Films 621(2017)98–101.
33. H. Ennaceri, M. Boujnah, A. Taleb, A. Khaldoun, R. Saez-Araoz, A. Ennaoui, A. El Kenz, A. Benyoussef. Thickness effect on the optical properties of TiO2-anatase thin films prepared by ultrasonic spray pyrolysis: Experimental and ab initio study. International journal of hydrogen energy 42 (2017) 19467–19480.
34. C. sahoo, a. k. gupta; and indu m. s. pillai. Photocatalytic degradation of methylene blue dye from aqueous solution using silver ion-doped TiO2 and its application to the degradation of real textile wastewater. Journal of Environmental Science and Health, Part A 47 (2012) 1428–1438.
35. R.S. Dariani, A. Esmaeili, A. Mortezaali, S. Dehghanpour. Photocatalytic reaction and degradation of methylene blue on TiO2 nano-sized particles. Optik 127 (2016) 7143–7154.
36. A. M. Tayeb, D. S. Hussein. Synthesis of TiO2 Nanoparticles and Their Photocatalytic Activity for Methylene Blue. American Journal of Nanomaterials, 3(2015)57–63.
37. B. Pal, R. Kaur, I. S. Grover. Superior Adsorption and Photodegradation of Eriochrome Black-T dye by Fe3+ and Pt4+ Impregnated TiO2 Nanostructures of Different Shapes. Journal of Industrial and Engineering Chemistry 33 (2016) 178–184
38. K. M. Reza, ASW Kurny and F. Gulshan. Parameters affecting the photocatalytic degradation of dyes using TiO2: a review. Appl Water Sci 7(2017)1569–1578.
39. U.G. Akpan, B.H. Hameed. Parameters affecting the photocatalytic degradation of dyes using TiO2-based photocatalysts: A review. Journal of Hazardous Materials 170 (2009) 520–529.
40. S. Ahmed, M.G. Rasul, W. M R. Brown and M. A. Hashib. The influence of Parameters on the Heterogeneous Photocatalytic Degradation of Pesticides and Phenolic Contaminants in Wastewater: A Short Review. Journal of Environmental Management 3 (2011) 311–330.
41. A. Kumar, G. Pandey. A Review on the Factors Affecting the Photocatalytic Degradation of Hazardous Materials. Material Science and Eengineering International Journal 1 (2017) 106- 114.
42. CC. Chan, CC. Chang, W. Hsu, S. Wang, J. Lin. Photocatalytic activities of Pd-loaded mesoporous TiO2 thin films. Chemical Engineering Journal 152 (2009) 492–497.
43. S. Sunasee, K. T. Wong, G. Lee, S. Pichiah, S. Ibrahim, C. Park, N. C. Kim, Y. Yoon, M. Jang. Titanium Dioxide-Based Sonophotocatalytic Mineralization of Bisphenol A and its Intermediates. Environmental Science and Pollution Research 24 (2017)15488–15488.
44. M. Capocelli, E. Joyce, A. Lancia, T. J. Mason, D. Musmarra, M. Prisciandaro. Sonochemical degradation of estradiol: Incidence of ultrasonic frequency. Chemical Engineering Journal 210 (2012) 9–17
45. K. Kang, M. Jangb, M. Cui, P. Qiu, S. Na, Y. Son, J. Khim. Enhanced sonocatalytic treatment of ibuprofen by mechanical mixing and reusable magnetic core titanium dioxide. Chemical Engineering Journal 264 (2015) 522–530.
46. M.S. Al-Amoudi, S.A. Bazaid, A.M.A. Adam, A. M. Asiri and M. Salman. Sono and Sonophotoctalysis for Wastewater Treatment. Der ChemicaSinica 3(2012) 129–147

47. A. Maezawa, H. Nakadoi, K. Suzuki, T. Furusawa and Y. Suzuki. Treatment of Dye Wastewater by using Photo-Catalytic Oxidation with Sonication, Shigeo Uchida. Ultrasonics Sonochemistry 14 (2007) 615–620.
48. M. Salehi, H. Hashemipour, M. Mirzaee. Experimental Study of In7luencing Factors and Kinetics in the Catalytic Removal of Methylene Blue with TiO2 Nanopowder. American Journal of Environmental Engineering 1(2012) 1–7.
49. E. Selli, C. L. Bianchi, C. Pirola, G. Cappelletti, V. Ragaini. Efficiency of 1,4-dichlorobenzene degradation in water under photolysis, photocatalysis on TiO2 and sonolysis. Journal of Hazardous Materials 153 (2008) 1136–1141
50. H. W. P. Carvalho, A. P. L. Batista, P. Hammer and T. C. Ramalho. Photocatalytic Degradation of Methylene blue by TiO2 –Cu Thin Films: Theoretical and Experimental Study. Journal of Hazardous Materials 184 (2010) 273–280.
51. E. Al-Hetlani, M.O. Amin, M. Madkour. Detachable photocatalysts of anatase TiO2 nanoparticles: Annulling surface charge for immediate photocatalyst separation. Applied Surface Science 411 (2017) 355–362
52. S. L. N. Zulmajdi, N. I. Zamri, A. H. Mahadi, M. Y. H. Rosli, F. Ja'afar, H. M. Yasin, E. Kusrini, J. Hobley, A. Usman. Sol-gel Preparation of Different Crystalline Phases of TiO2 Nanoparticles for Photocatalytic Degradation of Methylene Blue in Aqueous Solution. American Journal of Nanomaterials, 7(2019) 39–45.